PAPER

Check for updates

Design, synthesis and biological evaluation of N-arylsulfonyl carbazoles as novel anticancer agents†

Xin You,‡[a] Daqian Zhu,‡[ab] Wenhua Lu,[a] Yichen Sun,[a] Shuang Qiao,[ab] Bingling Luo,[ab] Yongliang Du,[ab] Rongbiao Pi,[b] Yumin Hu,[a] Peng Huang*[a] and Shijun Wen [ID] *[ab]

In this work, a set of structurally diverse synthetic carbazoles was screened for their anticancer activities. According to structure–activity relationship studies, carbazoles with an N-substituted sulfonyl group exhibited better anticancer activity. Moreover, compound **8h** was discovered to show the most potent anticancer effects on Capan-2 cells by inducing apoptosis and cell cycle arrest in G2/M phase. Finally, the in vivo study demonstrated that **8h** prevented the tumor growth in PANC-1 and Capan-2 xenograft models without apparent toxicity.

1. Introduction

Carbazoles and their derivatives are of great interest in the research fields of synthetic chemistry and medicinal chemistry, due to their tricyclic structure and widespread pharmacological properties.[1] In general, carbazoles constitute a useful class of polycyclic aromatic drugs displaying diverse activities including antibacterial,[2] neuroprotective,[3] anti-inflammatory,[4] antioxidant,[5] and anti-HIV functions.[6] More importantly, carbazoles are found to have effective antiproliferative activity on tumor cells (Fig. 1). Clausine B, a naturally occurring carbazole alkaloid, was found to be active (IC$_{50}$ < 30 μg mL^{-1}) against four human cancer cell lines including MDA-MB-231 (breast cancer), HeLa (cervical cancer), CAOV3 (ovarian cancer) and HepG2 (hepatic cancer).[7] Clausenawallines F showed cytotoxicity against oral cavity cancer (KB) and small-cell lung cancer (NCI-H187) with IC$_{50}$ values of 10.2 μM and 4.5 μM, respectively.[8] Due to the important pharmacological activities of the reported natural occurring carbazoles, an array of compounds containing carbazole motifs has been designed and synthesized for biological evaluation. For example, LY-333531 was reported as an anticancer agent by inhibiting Pim-1 kinase with IC$_{50}$ value of 0.2 μM.[9,10]

In the recent years, other research groups and ours have demonstrated that cyclic diphenyliodoniums (CDIs) are useful synthetic synthons for complex polycyclic arenes.[11–20] Due to the structural similarity of carbazoles and CDIs, it was envisioned that the insertion of nitrogen into the CDIs would be able to afford carbazoles. Indeed, we previously developed a synthetic strategy for carbazoles via the reaction of CDIs with various amines which was mediated by Cu(OAc)$_2$ at low cost.[11] With this strategy, an in-house chemical library of carbazoles with structural diversity and complexity was successfully built. The previous biological neuroprotective screening of the carbazole library found that some N-phenyl carbazoles showed good neuroprotection of neuronal cells HT22 against cell injury induced by glutamate or homocysteic acid.[12] Pancreatic cancer is one leading cause of cancer-related death and remains a serious clinical problem due to poor prognosis and the limited drug options.[21] In the continuation of our efforts to discover novel and potent anticancer agents, our in-house synthetic carbazoles were further screened for their potential antiproliferation of pancreatic cancer cells. The screening assay provided a structural starting point for further structure–activity study. In this work, we report the design and synthesis of structurally diversified carbazoles and their biological evaluation, leading to the discovery of novel N-arylsulfonyl carbazoles with both in vitro and in vivo antitumor therapeutic activities.

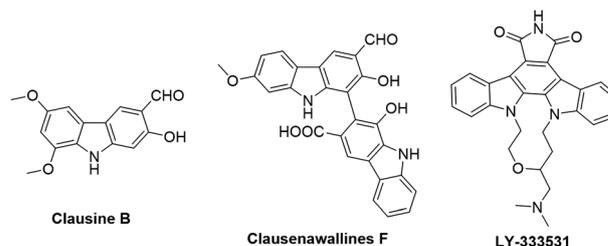[a]Sun Yat-sen University Cancer Center, State Key Laboratory of Oncology in South China, Collaborative Innovation Center for Cancer Medicine, Sun Yat-sen University, 651 Dongfeng East Road, Guangzhou 510060, China. E-mail: wenshj@sysucc.org.cn; huangpeng@sysucc.org.cn

[b]School of Pharmaceutical Sciences, Sun Yat-sen University, 132 Waihuan East Road, Guangzhou 510006, China

‡ Both authors contributed equally to this work.

Fig. 1 Representative carbazoles with anticancer activities.
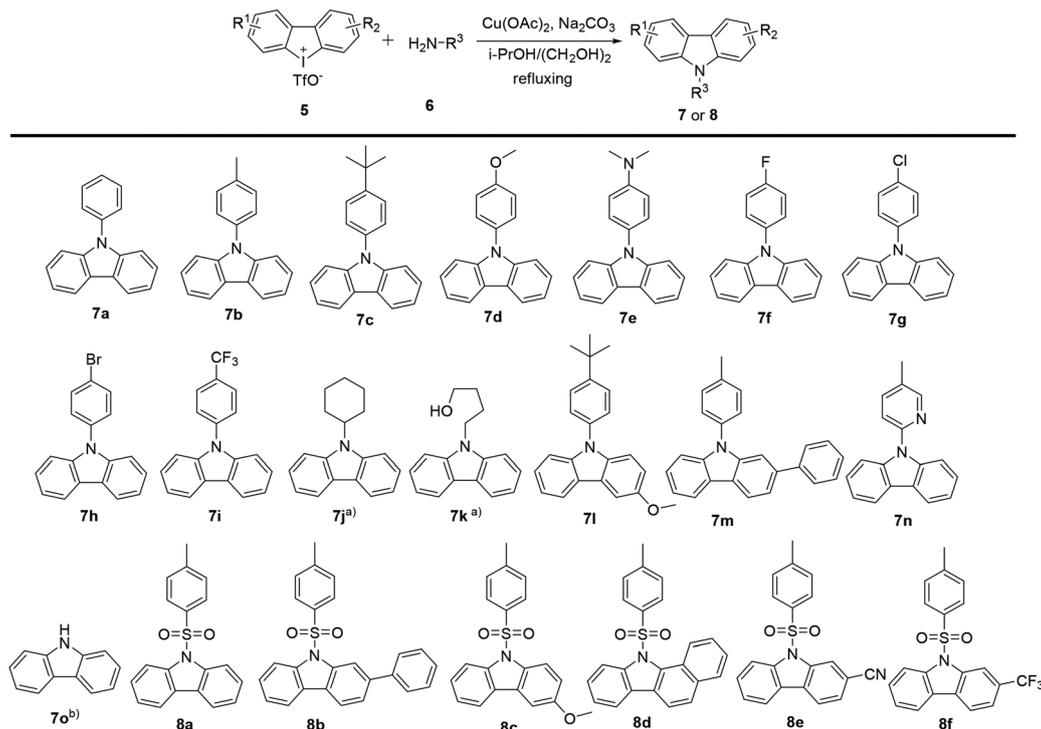
Scheme 1 Synthesis of carbazoles. Reaction conditions: diphenyleniodonium **5** (0.1 mmol), amine **6** (4 equiv.), Na$_2$CO$_3$ (3 equiv.), Cu(OAc)$_2$ (0.2 equiv.), 16 h, in refluxing i-PrOH/(CH$_2$OH)$_2$ (1.8/0.2 mL), argon atmosphere. (a) Additional CuI (0.2 equiv.) was added. (b) **7o** was obtained from the desulfonylation of **8a**.

2.   Results and discussion

2.1   Chemistry

2.1.1   General procedures for the synthesis of carbazoles with cyclic diphenyliodoniums. In previous work, we have demonstrated the construction of *N*-substituted carbazoles starting from cyclic diphenyl iodoniums.[11] The procedures for the synthesis of carbazoles were depicted in Scheme 1. The reactions of cyclic diphenyl iodoniums **5** with amines **6** were performed in a refluxing isopropanol/ethylene glycol (9/1) mixed solvent at argon atmosphere for 16 h, with Cu(OAc)$_2$ as the catalyst and Na$_2$CO$_3$ as the base. Thus, the reactions effectively afforded a series of *N*-aryl (**7a–7i** and **7l–7m**), *N*-pyridinyl (**7n**), *N*-aliphatic (**7j**, **7k**) and *N*-arylsulfonyl (**8a–8f**) substituted carbazoles at moderate to good yields. Besides, carbazole (**7o**) was also accessible after desulfonylation of **8a**. A mechanism study for this conversion was reported in our previous work.[11,12]

2.2   Biology

2.2.1   *In vitro* anticancer screening. The *in vitro* antitumor activities of the synthesized carbazole derivatives against human cancer cell lines, including two pancreatic cancer cell lines (PANC-1 and Capan-2), were assayed by MTS method. A summary of these results was shown in Table 1. *N*-Phenyl substituted carbazoles were found to display moderate to good neuroprotective activity by mediating ROS decrease in the neuronal cells HT22.[12] However, in this context, it was observed that the treatment with most of *N*-phenyl (**7a–7i** and **7l**, **7m**), *N*-

Table 1 The primary antiproliferative screening of **7a–7o** and **8a–8f** on PANC-1 and Capan-2 pancreatic cancer cell lines

Compound	Inhibitory rate of PANC-1 viability (%)		Inhibitory rate of Capan-2 viability (%)	
	30 μM	10 μM	30 μM	10 μM
7a	25.02	20.38	31.48	25.25
7b	12.59	16.42	21.01	23.82
7c	22.8	18.61	20.65	15.85
7d	25.9	17.65	34.8	12.91
7e	43.5	24.4	49.29	20.56
7f	11.75	34.27	22.55	28.82
7g	3.8	3.81	20.32	11.75
7h	71.1	19.05	38.12	18.58
7i	54.31	25.61	14.53	20.05
7j	19.78	18.18	15.93	32.61
7k	44.34	36.68	35.65	33.72
7l	5.4	23.76	35.98	30.36
7m	9.61	13.16	42.79	38.41
7n	34.73	33.84	24.94	20.91
7o	35.9	36.27	ND	27.03
8a	43.66	41.55	67.81	61.57
8b	59.8	63.98	70.54	66.79
8c	54.17	54.71	69.39	57.72
8d	53.92	34.94	72.62	72.04
8e	58.6	61.2	28.46	28.39
8f	56.67	48.05	82.2	66.6
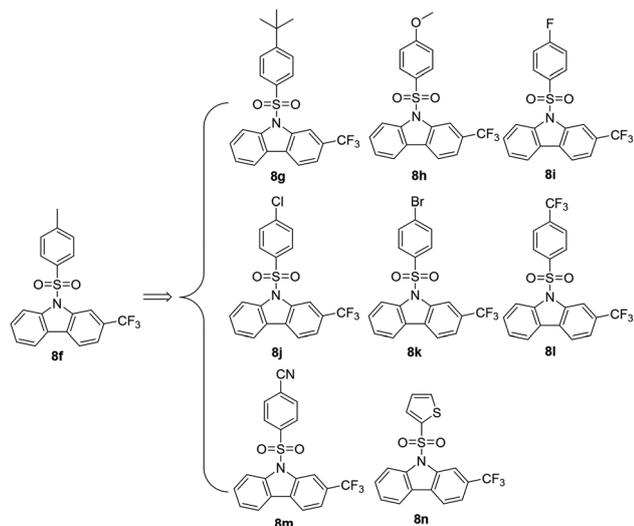
Scheme 2 Newly synthetic arylsulfonyl N-substituted carbazoles for more potent anticancer agents.

Table 2 The antiproliferative evaluation of **8g–8n** on PANC-1 and Capan-2 pancreatic cancer cell lines

	Inhibitory rate of PANC-1 viability (%)		Inhibitory rate of Capan-2 viability (%)	
Compound	30 μM	10 μM	30 μM	10 μM
8g	35.5	25.1	36.1	44.1
8h	**72.2**	**68.2**	**86.8**	**89.4**
8i	5.6	13.42	19.55	14.4
8j	36.8	16.5	58.7	52.4
8k	53.9	54.8	84.9	73.3
8l	43.3	8.49	29.7	31.41
8m	76.9	59.9	80.2	64.0
8n	61.6	57.3	40.4	49.1

pyridinyl (**7n**), N-aliphatic substituted carbazoles (**7j**, **7k**) and carbazole **7o** led to an inhibition of cell viability less than 50% at the tested concentrations. Thus, compounds **7a–7o** were excluded in further study, which was based on criterion of NCI-60 program.[22] Meanwhile, most of the N-arylsulfonyl substituted carbazoles (**8a–8f**) exhibited potent cytotoxic activities against PANC-1 and Capan-2 cell lines. Furthermore, among these effective carbazoles, different substituents on the carbazole motif and the N-sulfonyl group played a crucial role in

gaining antiproliferative activities. Carbazole with a trifluoromethyl (**8f**) was the best compared to the ones with alternative functional groups such as **8a**, **8c** (OMe), **8b** and **8d** (phenyl) and **8e** (CN).

2.2.2 Optimization of compound 8f. Based on the structure of **8f** (Scheme 2), a preliminary structure–activity relationship (SAR) study was conducted in order to find more potent agents, as shown in Table 2. In terms of substituents on the arylsulfonyl, tert-butyl (t-butyl, **8g**), methoxy (OMe, **8h**), and cyano (CN, **8m**) enhanced the anticancer efficiency. On the contrary, the carbazoles with an N-arylsulfonyl substituted by fluorine (F, **8i**), chlorine (Cl, **8j**) and trifluoromethyl (CF_3, **8l**) lost their anticancer efficacy drastically. Interestingly, the carbazole with an N-arylsulfonyl substituted by bromine (Br, **8k**) showed more effective cytotoxicity than its counterparts **8i** (–F) and **8j** (–Cl). A thiophenyl group to replace phenyl of arylsulfonyls did not help to improve the inhibitory effect of **8n** compared to the leading compound **8f**. It is worth mentioning that **8g–8n** were characterized by NMR and HRMS. Finally, the most potent compound **8h** was taken for further investigation for its antiproliferation against four different types of human cancer cell lines PANC-1 (pancreatic cancer), Capan-2 (pancreatic cancer), SGC-7901 (gastric cancer), HCT-116 (colon cancer), and HL-60 (leukemia), while 5-fluorouracil (5-FU) was selected as a positive control. As shown in the Table 3, **8h** demonstrated a broad spectrum of antitumor activities. Under our experiment conditions, the antiproliferative activities of **8h** were found to be more potent than 5-FU. Moreover, compound **8h** showed much lower toxicity (IC_{50}, 20.04 μM) to normal HFL-1 fibroblast cell line, indicating a good selectivity between human cancer and normal cells.

2.2.3 The effect of 8h on cell cycle of Capan-2 cancer cells. As a planar and aromatic polycyclic compound, carbazole derivative **8h** was reasoned to interact with DNA and induce a DNA damage.[23] Indeed, the treatment with **8h** in PANC-1 and Capan-2 cells increased the level of γ-H2AX protein, which is a sensitive molecular marker of DNA damage (Fig. 2A). Considering that DNA damage has been reported to induce cell cycle arrest,[24–26] the effect of **8h** on cell cycle distribution was also studied at different concentrations on Capan-2 cells. As shown in Fig. 2B–C, the treatment of Capan-2 cells at 5 μM resulted in more than 90% of the cells arrested in G2/M phase. The substantial accumulation of cancer cells in G2/M phase induced by **8h** might contribute to the antiproliferation of the compound.

Table 3 In vitro IC_{50} value (μM) of **8h** against tumor cell lines and normal cell line using MTS assay[a]

	Cell line (IC_{50} in μM)					
Compound	PANC-1	Capan-2	SGC-7901	HCT-116	HL-60	HFL-1
8h	3.69 ± 0.30	1.30 ± 0.28	2.25 ± 0.21	1.90 ± 0.14	2.20 ± 0.70	20.04 ± 2.48
5-Fu	19.31 ± 2.76	32.40 ± 3.70	16.56 ± 1.32	10.03 ± 0.88	NT	NT

[a] NT: not tested. Values are expressed as mean ± standard deviation (SD) of three independent duplicate experiments.
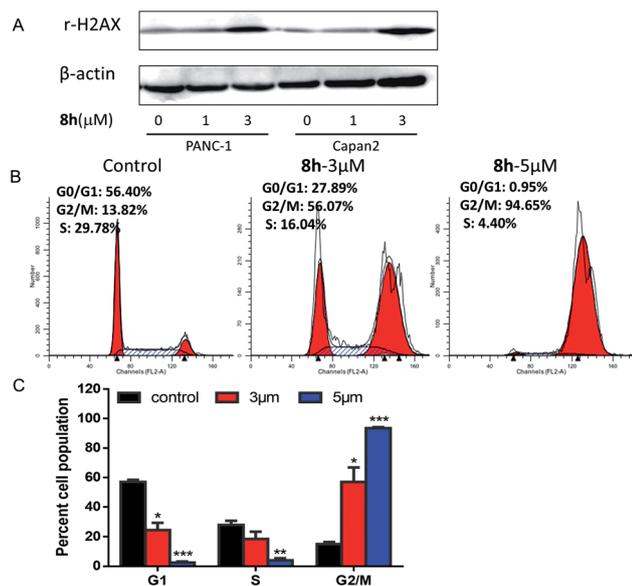
Fig. 2 Compound 8h induced DNA damage and cell cycle arrest in G2/M phase. (A) Protein γ-H2AX was analyzed by western blot. PANC-1 and Capan-2 cells were treated with 1 or 3 μM of compound 8h for 24 h. (B) Effect of compound 8h at 3 μM or 5 μM on the cell cycle of Capan-2 for 24 h. Cellular DNA contents were measured by PI staining using flow cytometry. The numbers indicate the normalization of each phase of cell cycle. (C) Histograms demonstrated the percentage of Capan-2 at different phases of the cell cycle. Error bars represent mean ± SD. *$p < 0.05$; **$p < 0.01$; ***$p < 0.001$.

2.2.4 The effect of 8h on the levels of cell-cycle regulatory proteins. To explore the potential molecular mechanism for 8h-induced cell cycle arrest at the G2/M phase, we examined the protein expression of cyclin B1 and phospho-Tyr15-Cdc2 which are crucial regulators in G2/M phase transition.[27,28] It is well known that the cell cycle is primarily regulated by CDK-cyclin complexes containing cyclin-dependent kinases (CDKs) and their cofactor cyclins.[29] The progression from G2 to mitosis is driven by the formation and activation of cdc2 (CDK1)-cyclin B1 complex.[30] As one of cdc2 negative regulator sites, Tyr15 phosphorylation inhibits cdc2 activity.[27] In PANC-1 and Capan-2 cells, 8h significantly decreased the expression level of cyclin B1 and increased the expression level of phospho-Tyr15-cdc2 (Fig. 3A–B), thus favoring cell cycle arrest at G2/M phase.

2.2.5 The effect of 8h on the apoptosis induction of Capan-2 cancer cells. We further investigated whether an induced apoptosis contributed to 8h's lethality by Annexin V-FITC and PI staining using flow cytometer. The apoptotic effect of compound 8h (3 μM and 5 μM) was evaluated on Capan-2 cells. Data indicated that 8h significantly increased the percentage of apoptotic cells in a dose-dependent manner compared to the control (Fig. 4A–B).

2.2.6 The role of ROS in mediating 8h-induced apoptosis. Reactive oxygen species (ROS) are well known to be a major player in redox signaling and a critical mediator of apoptosis.[31,32] The cancer cells in advanced stage tumors often exhibit high oxidative stress, suggesting that it might be possible to preferentially kill these cancer cells by
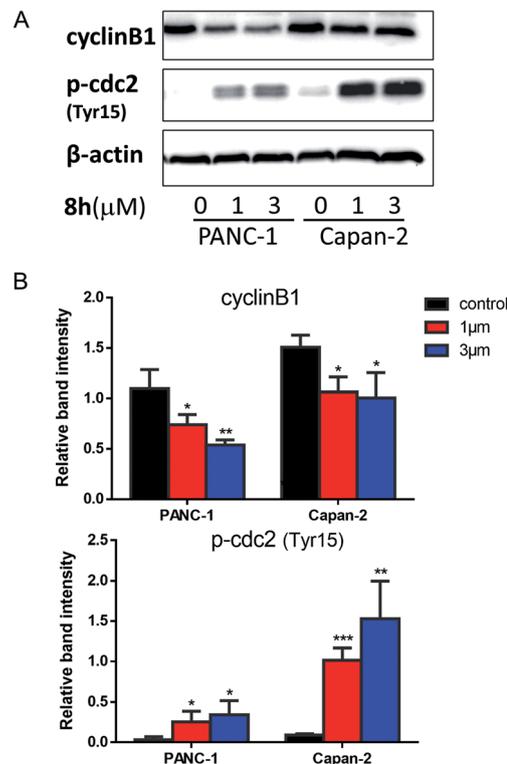

Fig. 3 The effect of compound 8h on the level of cyclin B1, p-Tyr15-cdc2. (A) Western blot was used to determine the expression of cyclin B1, p-Tyr15-cdc2 in PANC-1 and Capan-2 cells treated in the absence or presence (1 or 3 μM) of 8h for 24 h. (B) Densitometric analysis of cyclin B1, p-Tyr15-cdc2 proteins normalized with β-actin. The expression ratio of related proteins was quantified against β-actin using ImageJ software. Data were derived from three independent replicates. Bars means ± SD. *$p < 0.05$; **$p < 0.01$; ***$p < 0.001$.
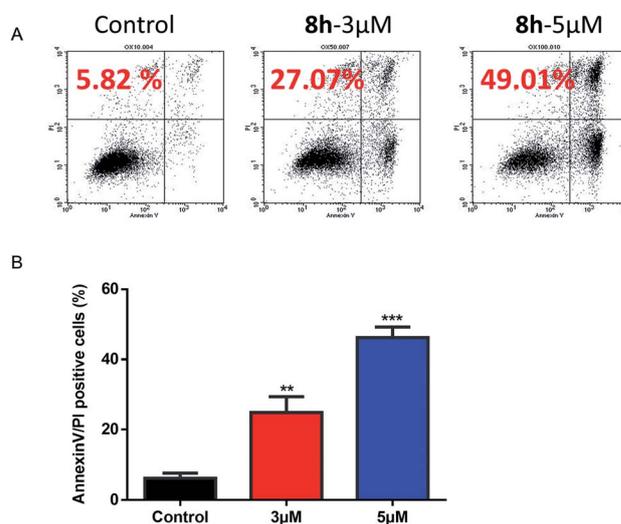
Fig. 4 Flow cytometric analysis of 8h induced apoptosis in Capan-2 cells using Annexin V-FITC and PI double staining. (A) Apoptosis rates were determined after Capan-2 cells were treated with 8h at 3 μM or 5 μM for 48 h. Percentage numbers indicate cell death population. (B) Percentage of Annexin V/PI positive cells were derived from three independent replicates. Data shown are mean values ± SD (error bar). **$p < 0.01$; ***$p < 0.001$.
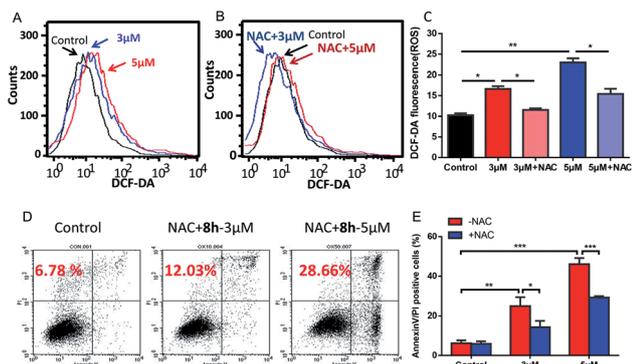
Fig. 5 Induction of ROS increase by compound **8h** and its partial reversion by an antioxidant NAC. (A) DCF-DA staining showed the effect of 3 μM (blue line) and 5 μM (red line) of **8h** on cellular ROS levels after 24 h treatment. (B and C) Pretreatment with NAC effectively reversed the ROS accumulation. Capan-2 cells were pre-treated with 3 mM NAC for 1 h and then incubated with compound **8h** (3 or 5 μM) for 24 h. Error bars represent mean ± SD. (D and E) Compound **8h**-induced apoptosis in Capan-2 cells was partially prevented by pre-treatment with NAC compared to Fig. 4. Capan-2 cells were pre-treated with 3 mM NAC for 1 h, and then incubated with the indicated concentrations (3 or 5 μM) of **8h** for 24 h. Error bars represent mean ± SD. $*p < 0.05$; $**p < 0.01$; $***p < 0.001$.

Fig. 6 *In vivo* antitumor effect of compound **8h** in PANC-1 xenograft model. **8h** was administered three times per week intraperitoneally at 40 mg kg^{-1} dosage. (A) Image of all dissected tumors. (B) The effect of **8h** on the PANC-1 tumor growth. (C) Tumor weight at day 28 after 4 weeks of treatment. (D) Mice weights were measured twice a week. Bars means ± SD. $**p < 0.01$; $***p < 0.001$.

pharmacologically increasing the ROS level transiently.[33] In previous work, we demonstrated that such strategy was effective to eliminate cancer cells by mediating intracellular ROS increase.[34,35] Therefore, it was of our interest whether such *N*-arylsulfonyl carbazole **8h** could elevate the intracellular ROS level in cancer cells. To test this possibility, the ROS level was measured when Capan-2 cells were subjected to **8h**. As shown in Fig. 5A–C, **8h** caused a concentration-dependent increase of cellular ROS, which could be partially reversed by pretreatment with an antioxidant *N*-acetyl-L-cysteine (NAC), a scavenger of ROS. Importantly, pretreatment with NAC also resulted in
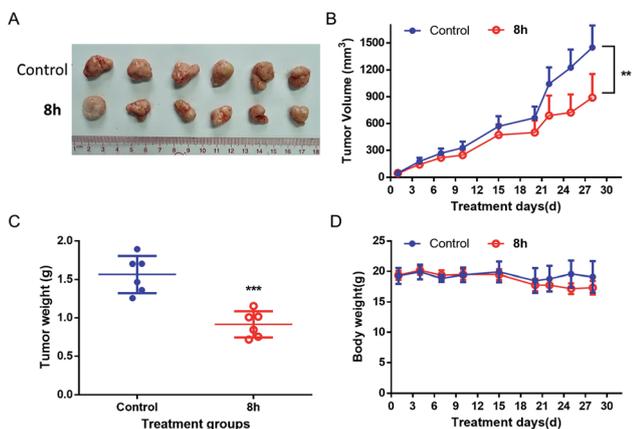

Fig. 7 *In vivo* antitumor effect of compound **8h** in Capan-2 xenograft model. **8h** was administered three times per week intraperitoneally at 40 mg kg^{-1} dosage. (A) Image of all dissected tumors. (B) The effect of 8 h on the Capan-2 tumor growth. (C) Tumor weight after 25 days of treatment. (D) Mice weights were measured twice a week. Bars means ± SD. $*p < 0.05$.

marked protection against **8h**-induced apoptosis (Fig. 5D–E), suggesting that the ROS generation induced by **8h** might play an important role in the cell apoptosis.

2.2.7   *In vivo* anticancer activity of 8h. Based on the promising *in vitro* anticancer activity of **8h** toward various cell lines, especially pancreatic cancer cell lines, we next evaluated *in vivo* anti-cancer activity of **8h** in PANC-1 and Capan-2 xenograft mice. Compared with the control group, PANC-1 tumor growth was substantially reduced in the mice treated with **8h** intraperitoneally three times weekly at a 40 mg kg^{-1} dosage, with approximately 40% volume inhibition (Fig. 6A–B). Furthermore, the treatment with **8h** for 28 days significantly diminished tumor weight (Fig. 6C). Meanwhile, no significant weight loss or illness was observed in the treatment group (Fig. 6D). Moreover, the anticancer effect of **8h** was also observed in another pancreatic cancer cell line Capan-2 xenograft mice (Fig. 7). Taken together, **8h** exhibited significant *in vivo* antitumor efficacy at a safe dose.
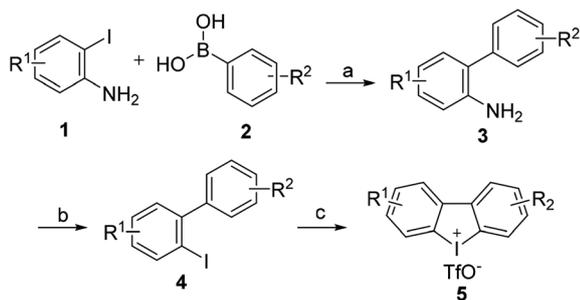
3.   Conclusions

In conclusion, a chemical library of *N*-substituted carbazoles was synthesized conveniently, and all the compounds were screened for a potential anticancer activity. Results demonstrated that the *N*-arylsulfonyl substituted carbazoles showed significant antiproliferative ability. A preliminary SAR study found that the synthetic compound **8h** displayed the most potent cytotoxic activity against PANC-1, Capan-2, SGC-7901, HCT-116, HL-60 cancer cells. Moreover, compound **8h** exhibited promising *in vivo* anticancer therapeutic efficacy in PANC-1 and Capan-2 xenograft mice models without an apparent side effect. The following preliminary investigation of its action model mechanism implied that the ROS mediated-apoptosis as well as the G2/M cell cycle arrest might contribute to the anticancer activity of **8h**. Environmentally benign and easily

Scheme 3 Synthesis of cyclic diphenyliodoniums (**5**). Reaction conditions: (a) Pd(PPh₃)₄, K₃PO₄, EtOH, reflux, 6 h. (b) (i). NaNO₂, 0 °C THF, 4 M HCl, (ii). KI, rt. (c) mCPBA (85%), TfOH, CH₂Cl₂, rt, 2 h.

accessible synthesis and the potent anticancer activity may make these *N*-arylsulfonyl substituted carbazoles to be promising drug candidates to kill cancer cells.

4. Experiments

4.1 Chemistry

4.1.1 General information. All solvents were commercially available and were used without a further purification unless stated. The chemicals used were either purchased from commercial sources or prepared according to literature procedures. The ^{1}H and ^{13}C nuclear magnetic resonance (NMR) spectra were recorded on a Bruker Avance spectrometer 400 at 400 and 100 MHz respectively. Chemical shifts are given in ppm (δ) referenced to CDCl₃ with 7.26 for ^{1}H and 77.10 for ^{13}C, and to d_6-DMSO with 2.50 for ^{1}H and 39.52 for ^{13}C. In the case of multiplet, the signals are reported as intervals. Signals are abbreviated as follows: s, singlet; d, doublet; t, triplet; q, quartet; m, multiplet. Coupling constants are expressed in hertz. The progress of the reactions was monitored by thin-layer chromatography on a glass plate coated with silica gel with fluorescent indicator (GF254). Column chromatography was performed on silica gel (200–300 mesh).

4.1.2 General procedures for the synthesis of cyclic diphenyleneiodoniums. The procedures[11] for the synthesis of cyclic diphenyliodoniums **5** were depicted in Scheme 3. Catalyzed by Pd(PPh₃)₄, substituted 2-iodoaniline **1** reacted with functionalized phenlyboronic acid **2** yielded areneamine **3** at a good yield. **3** was readily transformed into iodoarene **4** *via* a Sandermeyer reaction, and then cyclic diphenyliodoniums **5** could be obtained after **4** was treated with mCPBA and triflic acid (TfOH) for 2 h at room temperature.

4.1.3 Synthesis and characterization of the carbazole derivatives.
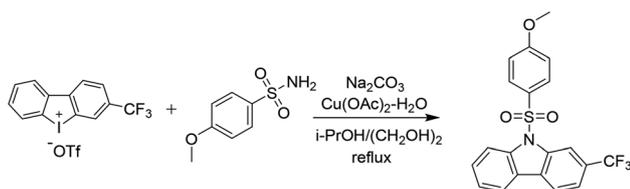
The general procedure for the preparation of these carbazoles was exemplified by the synthesis of **8h**:

To a stirred solution of 3-(trifluoromethyl)dibenzo[*b,d*]iodol-5-ium trifluoromethanesulfonate (100 mg, 0.2 mmol, 1 eq.) in i-PrOH (1.8 mL) and ethylene glycol (0.2 mL), was added 4-methoxybenzenesulfonamide (151 mg, 0.8 mmol, 4 equiv.), sodium carbonate (64 mg, 0.6 mmol, 3 equiv.), Cu(OAc)₂ (8 mg, 0.04 mmol, 0.2 equiv.). The reaction proceeded at a reflux for 16 h under argon atmosphere before i-PrOH was removed by a rotary evaporation. The remained mixture was partitioned between water and EtOAc, and the aqueous phase was extracted with EtOAc. The combined organic phases were washed with H₂O and brine, dried over anhydrous Na₂SO₄, evaporated in a *vacuo*. The residue was purified by column chromatography on a silica gel (PE/EtOAc = 15/1–5/1) to provide carbazole **8h**.

4.1.3.1   9-((4-(tert-Butyl)phenyl)sulfonyl)-2-(trifluoromethyl)-9H-carbazole (8g). A white solid, 63% yield. ^{1}H NMR (400 MHz, CDCl₃) δ 8.65 (s, 1H), 8.37 (d, *J* = 8.4 Hz, 1H), 8.00 (dd, *J* = 16.8, 7.9 Hz, 2H), 7.77 (d, *J* = 8.7 Hz, 2H), 7.63 (d, *J* = 8.0 Hz, 1H), 7.58 (t, *J* = 7.9 Hz, 1H), 7.42 (t, *J* = 7.5 Hz, 1H), 7.37 (d, *J* = 8.7 Hz, 2H), 1.21 (s, 9H). ^{13}C NMR (100 MHz, CDCl₃) δ 158.3, 139.3, 137.9, 134.9, 128.8, 126.6, 126.5, 125.2, 124.3, 120.8, 120.5, 115.3, 112.5, 35.4, 31.0 ppm. HRMS calcd for C₂₃H₂₀F₃NO₂S [M + H]⁺: 432.1245, found: 432.1239.

4.1.3.2   9-((4-Methoxyphenyl)sulfonyl)-2-(trifluoromethyl)-9H-carbazole (8h). A white solid, 69% yield. ^{1}H NMR (400 MHz, CDCl₃) δ 8.63 (s, 1H), 8.36 (d, *J* = 8.5 Hz, 1H), 7.98 (dd, *J* = 17.1, 8.0 Hz, 2H), 7.76 (d, *J* = 8.9 Hz, 2H), 7.62 (d, *J* = 8.0 Hz, 1H), 7.57 (t, *J* = 7.4 Hz, 1H), 7.41 (t, *J* = 7.5 Hz, 1H), 6.79 (d, *J* = 8.9 Hz, 2H), 3.74 (s, 3H). ^{13}C NMR (100 MHz, CDCl₃) δ 164.2, 139.3, 137.9, 129.4, 129.2, 128.8, 128.7, 125.9, 125.2, 124.3, 123.1, 120.8, 120.5, 115.3, 114.5, 112.6, 112.5, 55.7 ppm. HRMS calcd for C₂₀H₁₄F₃NO₃S [M + H]⁺: 406.0724, found: 406.0721.

4.1.3.3   9-((4-Fluorophenyl)sulfonyl)-2-(trifluoromethyl)-9H-carbazole (8i). A white solid, 46% yield. ^{1}H NMR (400 MHz, CDCl₃) δ 8.61 (s, 1H), 8.34 (d, *J* = 8.3 Hz, 1H), 7.99 (dd, *J* = 17.7, 7.9 Hz, 2H), 7.89–7.78 (m, 2H), 7.65 (d, *J* = 7.9 Hz, 1H), 7.59 (t, *J* = 7.9 Hz, 1H), 7.44 (t, *J* = 7.3 Hz, 1H), 7.03 (t, *J* = 7.8 Hz, 2H). ^{13}C NMR (100 MHz, CDCl₃) δ 167.3, 164.8, 139.2, 137.8, 133.6, 133.6, 129.7, 129.5, 129.4, 129.0, 125.8, 125.4, 124.7, 123.1, 120.9, 120.6, 116.9, 116.7, 115.3, 112.6, 112.5 ppm. HRMS calcd for C₁₉H₁₁F₄NO₂S [M − H]⁻: 392.0369, found: 392.0371.

4.1.3.4   9-((4-Chlorophenyl)sulfonyl)-2-(trifluoromethyl)-9H-carbazole (8j). A white solid, 52% yield. ^{1}H NMR (400 MHz, CDCl₃) δ 8.60 (s, 1H), 8.33 (d, *J* = 8.4 Hz, 1H), 7.99 (dd, *J* = 18.1, 8.0 Hz, 2H), 7.74 (d, *J* = 8.5 Hz, 2H), 7.65 (d, *J* = 8.0 Hz, 1H), 7.58 (t, *J* = 7.8 Hz, 1H), 7.44 (t, *J* = 7.5 Hz, 1H), 7.32 (d, *J* = 8.6 Hz, 2H). ^{13}CNMR (100 MHz, CDCl₃) δ 141.1, 139.2, 137.8, 136.0, 129.7, 129.4, 129.0, 128.0, 125.4, 124.8, 121.3, 121.3, 121.0, 120.7, 115.3, 112.6, 112.6 ppm. HRMS calcd for C₁₉H₁₁ClF₃NO₂S [M + H]⁺: 410.0029, found: 410.0028.

4.1.3.5   9-((4-Bromophenyl)sulfonyl)-2-(trifluoromethyl)-9H-carbazole (8k). A white solid, 49% yield. ^{1}H NMR (400 MHz, CDCl₃) δ 8.59 (s, 1H), 8.33 (d, *J* = 8.5 Hz, 1H), 7.99 (dd, *J* = 17.9, 8.0 Hz, 2H), 7.66 (d, *J* = 8.7 Hz, 3H), 7.58 (t, *J* = 7.8 Hz, 1H), 7.48 (d, *J* = 8.7 Hz, 2H), 7.44 (t, *J* = 7.5 Hz, 1H). ^{13}C NMR (100 MHz, CDCl₃) δ 139.2, 137.8, 136.5, 132.7, 129.7, 129.5, 129.0, 128.0,

125.5, 124.8, 121.3, 121.0, 120.7, 115.4, 112.6 ppm. HRMS calcd for $C_{19}H_{11}BrF_3NO_2S$ $[M + H]^+$: 453.9724, found: 453.9718.

4.1.3.6 2-(Trifluoromethyl)-9-((4-(trifluoromethyl)phenyl) sulfonyl)-9H-carbazole (8l). A white solid, 57% yield. ^1H NMR (400 MHz, CDCl$_3$) δ 8.61 (s, 1H), 8.35 (d, $J = 8.5$ Hz, 1H), 8.00 (dd, $J = 18.5$, 7.9 Hz, 2H), 7.93 (d, $J = 8.1$ Hz, 2H), 7.67 (d, $J = 8.1$ Hz, 1H), 7.64–7.57 (m, 3H), 7.45 (t, $J = 7.6$ Hz, 1H). ^{13}C NMR (100 MHz, CDCl$_3$) δ 140.9, 139.1, 137.7, 136.0, 135.7, 129.9, 129.5, 129.1, 127.2, 126.6, 126.6, 125.7, 125.5, 125.0, 124.3, 123.0, 121.5, 121.0, 120.8, 115.3, 112.6, 112.5 ppm. HRMS calcd for $C_{20}H_{11}F_6NO_2S$ $[M - H]^-$: 442.0337, found: 442.0335.

4.1.3.7 4-((2-(Trifluoromethyl)-9H-carbazol-9-yl)sulfonyl)benzonitrile (8m). A white solid, 51% yield. ^1H NMR (400 MHz, CDCl$_3$) δ 8.58 (s, 1H), 8.32 (d, $J = 8.4$ Hz, 1H), 8.00 (dd, $J = 18.6$, 7.9 Hz, 2H), 7.89 (d, $J = 8.6$ Hz, 2H), 7.67 (d, $J = 8.2$ Hz, 1H), 7.63 (dd, $J = 7.6$, 5.0 Hz, 2H), 7.62–7.57 (m, 1H), 7.46 (t, $J = 7.6$ Hz, 1H). ^{13}C NMR (100 MHz, CDCl$_3$) δ 141.2, 138.9, 137.6, 133.2, 130.0, 129.6, 129.2, 127.2, 125.6, 125.2, 121.7, 121.7, 121.1, 120.8, 118.1, 116.8, 115.3, 112.6, 112.6 ppm. HRMS calcd for $C_{20}H_{11}F_3N_2O_2S$ $[M - H]^-$: 399.0415, found: 399.0415.

4.1.3.8 9-(Thiophen-2-ylsulfonyl)-2-(trifluoromethyl)-9H-carbazole (8n). A white solid, 72% yield. ^1H NMR (400 MHz, CDCl$_3$) δ 8.61 (s, 1H), 8.35 (d, $J = 8.5$ Hz, 1H), 8.00 (dd, $J = 16.7$, 7.8 Hz, 2H), 7.66 (d, $J = 8.1$ Hz, 1H), 7.63–7.56 (m, 2H), 7.48–7.42 (m, 2H), 6.92 (dd, $J = 5.0$, 3.9 Hz, 1H). ^{13}C NMR (100 MHz, CDCl$_3$) δ 139.0, 137.6, 136.9, 133.4, 132.9, 129.5, 129.2, 128.8, 127.5, 125.7, 125.4, 124.7, 123.0, 121.1, 120.7, 120.4, 115.5, 112.8 ppm. HRMS calcd for $C_{17}H_{10}F_3NO_2S_2$ $[M + H]^+$: 382.0183, found: 382.0181.

4.2 Biological assay

4.2.1 Cell lines and cell culture. Human cell lines Capan-2 (pancreatic cancer) and HCT-116 (colon cancer) were purchased from American Tissue Culture Collection (Manassas, VA, USA). Cell lines PANC-1 (pancreatic cancer), SGC-7901 (gastric cancer), HL-60 (leukemia) and HFL-1 (normal human lung fibroblast) were purchased from the cell bank, Chinese Academy of Sciences (Shanghai, China). The medium for cell culture were specified by the instructions of cell repository banks. All medium were obtained from Invitrogen Life Technologies (Carlsbad, CA, USA) and supplemented with 10% fetal bovine serum (GIBCO, Carlsbad, CA, USA). All cell lines were cultured at 37 °C in a humidified incubator with 5% CO$_2$ atmosphere.

4.2.2 MTS assay. Cell viability was determined by MTS assay (Promega, Madison, WI, USA).[36] Cells were seeded in a 96-well plate at a density of 3000 cells per well. We simultaneously prepared blank wells containing media only. The stock solutions of test compounds were dissolved in appropriate volume so that the final DMSO concentration during treatment in cells was not more than 0.1%. Treated cells were cultured with indicated compounds while control cells were treated with 0.1% (v/v) DMSO. After 72 h of treatment, 20 µL MTS reagent was added to each well and incubated for an additional 4 hours at 37 °C. The optical density (OD) was determined by microplate reader (Thermo, Helsinki, Finland) at 490 nm. The experiment

was repeated for three independent times. The percentages of cell viability and inhibitory rate of cell viability were calculated using formulas:

$$\text{Cell viability \%} = \frac{\text{OD value of treated cells} - \text{OD value of blank}}{\text{OD value of control cells} - \text{OD value of blank}} \times 100$$

$$\text{Inhibitory rate of cell viability (\%)} = 100 - \text{cell viability (\%)}$$

4.2.3 Cell cycle analysis. Cells were seeded in 6-well plates with a density of 2×10^5 cells per well and incubated with different concentrations of drugs for 24 h. The cells were harvested and fixed with 70% alcohol at 4 °C for 2 h and then incubated with RNase at 37 °C for 30 min followed by addition of PI. Finally, cell cycle distribution was detected using FACS Calibur flow cytometer (BD Biosciences).

4.2.4 Apoptosis assay. Apoptosis was detected by an Annexin-V/PI assay kit (KeyGEN, Nanjing, China). After the drug treatment, cells were harvested and washed. The cells were then stained with Annexin-V-FITC and propidium iodide (PI) in binding buffer for 15 min and apoptotic rates were analyzed using FACS flow cytometer (BD Biosciences, San Diego, CA, USA). Comparisons between groups were tested by one-way ANOVA analysis.

4.2.5 Analysis of ROS. Cells were seeded in six-well plates at 2×10^5 cells per well overnight and treated with compound **8h** at indicated concentrations for 24 h. Then the cells were collected and stained with CMH2DCF-DA (Sigma-Aldrich) followed by flow cytometry analysis using FACS Calibur flow cytometer (BD Biosciences). In some experiments of ROS analysis, cells were pre-treated with 3 mM NAC (Sigma-Aldrich, St. Louis, MO, USA) for 1 h prior to the exposure to compound **8h**. Statistical comparisons were analyzed by one-way ANOVA.

4.2.6 Western blot analysis. Collected cells were homogenized in lysis buffer (5% SDS, 10 mM EDTA, 50 mM NaCl, 10 mM Tris–HCl). Protein concentrations were measured using pierce BCA protein assay (Thermo Fisher, Rockford, IL, USA). Proteins were run on a standard SDS-PAGE and transferred to PVDF membranes. Membranes were blocked in 5% milk, incubated with primary antibody at a concentration of 1 : 1000, then incubated with secondary antibody at a concentration of 1 : 10 000 and read using ECL detection system (Bio-Rad, Richmond, CA). β-Actin was used as a loading control. Anti-γ-H2AX (phospho-Ser139), anti-cyclinB1, anti-phospho-cdc2 (Tyr15), and anti-β-actin were purchased from Cell Signaling Technology (Danvers, MA, USA). The expression ratio of cyclinB1 and p-cdc2 (Tyr15) proteins was quantified against β-actin using ImageJ software. One-way ANOVA was used for statistical analysis.

4.2.7 Animal study. The exponentially growing PANC-1 and Capan-2 cells were collected and injected subcutaneously into the flanks of 5 week-old female immune-deficient BALB/c nude mice (Vital River, Beijing, China) at 2×10^6 cells or 3×10^6 cells

per injection site respectively. After the formation of palpable tumors, the nude mice were randomly assigned into control and treatment groups (six mice per group). Compound **8h** was dissolved in 80% PBS, 10% DMSO and 10% cremophor and administered intraperitoneally three times weekly at a dose of 40 mg kg^{-1}. Control mice were treated with equal volume of vehicle (80% PBS, 10% DMSO and 10% cremophor). The mice body weight and tumor volume, which was calculated by the formula $0.5 \times$ length $\times$ width^2 were measured twice a week. At the end of the experiment, the mice were sacrificed, their tumors were dissected, and the tumor weights were measured. p values were calculated using the two-tailed Student t-test. The animal study was conducted in accordance with a protocol approved by the Institutional Animals Care and Use Committee of Sun Yat-sen University Cancer Center. The code for IACUC approval was L102012016020G.

4.2.8 Statistical analysis. Data were presented as mean $\pm$ SD. The statistical significance of differences was determined using the Student's t-test or one-way ANOVA. p value < 0.05 was regarded as statistically significant.

Conflicts of interest

There are no conflicts to declare.

Acknowledgements

References

1 A. W. Schmidt, K. R. Reddy and H. J. Knolker, *Chem. Rev.*, 2012, **112**, 3193–3328.

2 P. Y. Wang, H. S. Fang, W. B. Shao, J. Zhou, Z. Chen, B. A. Song and S. Yang, *Bioorg. Med. Chem. Lett.*, 2017, **27**, 4294–4297.

3 A. A. Pieper, S. Xie, E. Capota, S. J. Estill, J. Zhong, J. M. Long, G. L. Becker, P. Huntington, S. E. Goldman, C. H. Shen, M. Capota, J. K. Britt, T. Kotti, K. Ure, D. J. Brat, N. S. Williams, K. S. MacMillan, J. Naidoo, L. Melito, J. Hsieh, J. De Brabander, J. M. Ready and S. L. McKnight, *Cell*, 2010, **142**, 39–51.

4 A. D. Favia, D. Habrant, R. Scarpelli, M. Migliore, C. Albani, S. M. Bertozzi, M. Dionisi, G. Tarozzo, D. Piomelli, A. Cavalli and M. De Vivo, *J. Med. Chem.*, 2012, **55**, 8807–8826.

5 D. Pratico, *Trends Pharmacol. Sci.*, 2008, **29**, 609–615.

6 K. M. Meragelman, T. C. McKee and M. R. Boyd, *J. Nat. Prod.*, 2000, **63**, 427–428.

7 W. N. Wan Mohd Zain, A. Rahmat, F. Othman and T. Y. Yap, *Malays J Med Sci*, 2009, **16**, 29–34.

8 W. Maneerat, T. Ritthiwigrom, S. Cheenpracha, T. Promgool, K. Yossathera, S. Deachathai, W. Phakhodee and S. Laphookhieo, *J. Nat. Prod.*, 2012, **75**, 741–746.

9 R. Akue-Gedu, E. Rossignol, S. Azzaro, S. Knapp, P. Filippakopoulos, A. N. Bullock, J. Bain, P. Cohen, M. Prudhomme, F. Anizon and P. Moreau, *J. Med. Chem.*, 2009, **52**, 6369–6381.

10 D. Drygin, M. Haddach, F. Pierre and D. M. Ryckman, *J. Med. Chem.*, 2012, **55**, 8199–8208.

11 D. Zhu, Q. Liu, B. Luo, M. Chen, R. Pi, P. Huang and S. Wen, *Adv. Synth. Catal.*, 2013, **355**, 2172–2178.

12 D. Zhu, M. Chen, M. Li, B. Luo, Y. Zhao, P. Huang, F. Xue, S. Rapposelli, R. Pi and S. Wen, *Eur. J. Med. Chem.*, 2013, **68**, 81–88.

13 D. Zhu, Y. Wu, B. Wu, B. Luo, A. Ganesan, F. H. Wu, R. Pi, P. Huang and S. Wen, *Org. Lett.*, 2014, **16**, 2350–2353.

14 Z. Liu, D. Zhu, B. Luo, N. Zhang, Q. Liu, Y. Hu, R. Pi, P. Huang and S. Wen, *Org. Lett.*, 2014, **16**, 5600–5603.

15 M. Wang, S. Chen and X. Jiang, *Org. Lett.*, 2017, **19**, 4916–4919.

16 M. Wang, Q. Fan and X. Jiang, *Org. Lett.*, 2018, **20**, 216–219.

17 M. Wang, J. Wei, Q. Fan and X. Jiang, *Chem. Commun.*, 2017, **53**, 2918–2921.

18 Q. Tan, D. Zhou, T. Zhang, B. Liu and B. Xu, *Chem. Commun.*, 2017, **53**, 10279–10282.

19 S. Riedmuller and B. J. Nachtsheim, *Beilstein J. Org. Chem.*, 2013, **9**, 1202–1209.

20 H. Xie, M. Ding, M. Liu, T. Hu and F. Zhang, *Org. Lett.*, 2017, **19**, 2600–2603.

21 A. P. Klein, *Nat. Rev. Cancer*, 2013, **13**, 66–74.

22 In *Anticancer Drug Development Guide: Preclinical Screening, Clinical Trials, and Approval*, ed. B. A. Teicher and P. A. Andrews, Humana press, Totowa, NJ, 2004, pp. 41–62.

23 C. Asche and M. Demeunynck, *Anti-Cancer Agents Med. Chem.*, 2007, **7**, 247–267.

24 M. Laiho and L. Latonen, *Ann. Med.*, 2003, **35**, 391–397.

25 K. Ishikawa, H. Ishii and T. Saito, *DNA Cell Biol.*, 2006, **25**, 406–411.

26 I. A. Shaltiel, L. Krenning, W. Bruinsma and R. H. Medema, *J. Cell Sci.*, 2015, **128**, 607–620.

27 R. Y. Zhao and R. T. Elder, *Cell Res.*, 2005, **15**, 143–149.

28 L. Tang, Y. Zhang, H. Pan, Q. Luo, X. M. Zhu, M. Y. Dong, P. C. Leung, J. Z. Sheng and H. F. Huang, *Reprod. Biol. Endocrinol.*, 2009, **7**, 144.

29 S. Lim and P. Kaldis, *Development*, 2013, **140**, 3079–3093.

30 T. Miyazaki and S. Arai, *Cell Cycle*, 2007, **6**, 1419–1425.

31 J. M. Mates, J. A. Segura, F. J. Alonso and J. Marquez, *Arch. Toxicol.*, 2012, **86**, 1649–1665.

32 K. Sinha, J. Das, P. B. Pal and P. C. Sil, *Arch. Toxicol.*, 2013, **87**, 1157–1180.

33 D. Trachootham, J. Alexandre and P. Huang, *Nat. Rev. Drug Discovery*, 2009, **8**, 579–591.

34 J. Wang, B. Luo, X. Li, W. Lu, J. Yang, Y. Hu, P. Huang and S. Wen, *Cell Death Dis.*, 2017, **8**, e2887.

35 D. Trachootham, Y. Zhou, H. Zhang, Y. Demizu, Z. Chen, H. Pelicano, P. J. Chiao, G. Achanta, R. B. Arlinghaus, J. Liu and P. Huang, *Cancer Cell*, 2006, **10**, 241–252.

36 A. M. Schrand, J. B. Lin and S. M. Hussain, *Methods Mol. Biol.*, 2012, **906**, 395–402.